02

Influence of radiation defects of different type on the critical current of layered anisotropic superconductor

© A.N. Maksimova, V.A. Kashurnikov, A.N. Moroz, I.A. Rudnev

National Research Nuclear University„MEPhI“,
Moscow, Russia

E-mail: anmaksimova@mephi.ru

Received July 16, 2021
Revised July 16, 2021
Accepted July 18, 2021

The effect of radiation defects on the critical current of a layered anisotropic superconductor has been investigated by numerical methods. Model defects simulating various cases of radiation damage to a superconductor as a result of electron and ion irradiation are considered. The obtained dependences of the critical current on the magnetic field show that the greatest pinning gain with equal irradiation fluence is given by defects forming 3D conical regions inside the superconductor. It is shown that in a weakly anisotropic superconductor, conical defects enhance the critical current more efficiently than in a strongly anisotropic one. The interaction of a vortex lattice with radiation defects is considered, vortex configurations arising under the action of the self-field of the transport current are obtained.

Keywords: HTSC, pinning, Abrikosov vortices, radiation defects, Monte Carlo method.

DOI: 10.21883/PSS.2022.13.52308.169

1. Introduction

Despite the significant amount of studies, the rise of pinning in a high-temperature superconductor (HTSC) remains an important task. Modern HTSC tapes of the second generation, for example, based on rare earth compounds (*Re*BaCuO, where *Re* — rare earth), have high critical currents, due to which they are widely used in the electric power industry, allowing to create highly efficient power transmission lines, motors and generators. HTSC tapes also have the ability to maintain a high critical current in magnetic fields, that allows to use them in accelerators and tokamaks, where they are exposed to radiation. Experimental studies show, that under the action of radiation in a superconductor, defects of various types are formed, which can be pinning centers for vortices. Thus, radiation affects superconductor magnetic and transport properties, and this also means the ability to change the sample properties by purposefully irradiating it with particles of various types. In practice irradiation with neutrons [1], protons [2], electrons [3], γ-quanta [4] and heavy ions [5] is used. In this case the defect shape depends on the energy and type of the irradiating particles. When irradiated with electrons and γ-quanta, predominantly point pinning centers arise; when irradiated with heavy ions, the shape can be either in the shape of a rectilinear track with a radius of the order of the coherence length (ion energy in the range from hundreds of MeV to several GeV), as well as an area of considerable size (cascade), that does not penetrate through the film. Such a defect arises, in case irradiating ion energy is less than or of the order of several MeV per nucleon [6], and HTSC layer thickness is greater than the projective range of the ions. The character of defect formation in HTSC can be estimated by means of the widely used SRIM (Stopping and Range of Ions in Matter) package [7]. For example, [8] presents the results of calculating the concentration of radiation defects in HTSC for some types of ions. Approximately, in a numerical calculation, a cascade of defects can be considered as a model of a cone with a vertex on the film surface. The depth of such a defect depends on the irradiating ion energy and, therefore, can be controlled.

As numerous studies show, irradiation at low fluences can result in both rise and fall of the critical current. In practice, the situation depends on the value of initial critical current of the superconductor, as well as irradiation type and fluence. The rise of critical current with an increase of the defect concentration (Fig. 1) is associated with the formation of new pinning centers, a decrease is due to a number of factors that will be described below. Although in this article we are interested in the first region — the rise of critical current, we will briefly review the experimental data concerning both the first and the second area.

In the studies [9–15] the degradation of the superconducting HTSC tape properties under neutron irradiation was investigated. It was found that tapes degrade faster at high operating temperatures and in a magnetic field parallel to the tape plane. It is also shown that at a low irradiation fluence, an increase of critical current is observed, which at a certain value ($1.2 \cdot 10^{22}\,\mathrm{m}^{-2}$) reaches a maximum. The effect of neutron irradiation on HTSC tapes containing artificial pinning centers was carried out in the study [14]. It is shown that the drop in the critical temperature is

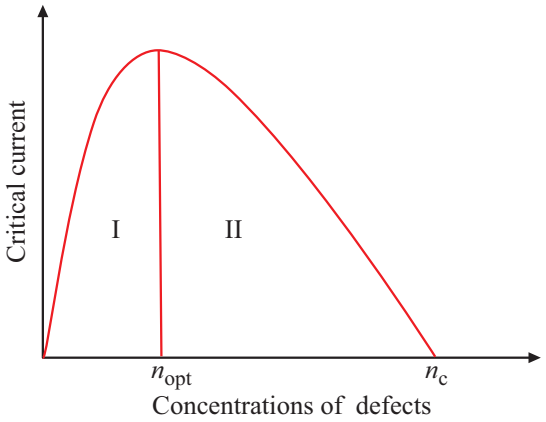

Figure 1. Qualitative dependence of critical current on the defect concentration for type II superconductors. I — area of critical current rise, II — area critical current fall.

determined only by the fluence and does not depend on the presence of artificial defects, while the critical current in the presence of artificial defects degrades at a lower fluence. It is also shown that at high fluences($2.3 \cdot 10^{22}\,m^{-2}$), the bulk vortex pinning is determined only by radiation defects.

If during irradiation for small fluences the growth of critical current is observed, then upon reaching a certain, depending on a particular superconductor, irradiation fluence (for example, for irradiation $YBa_2Cu_3O_{7+\delta}$ (YBCO) by fast neutrons this value is $\sim 10^{22}\,m^{-2}$ [14], see also [15]) the growth of critical current is replaced by its degradation. This is partly due to a decrease of critical temperature with a growth of defect concentration, partly — with the overlap of their potential pits [16]. Also the irreversibility field [14] is subject to the same dependence on radiation. Another effect is the adjustment of the vortex lattice to the defect lattice ([17], where minima were observed in the dependence of the magnetoresistance on the external field at tuning fields). In [18] the effect of irradiation on the relaxation rate in the superconductor $CaFe_2As_2$ was investigated. The influence of irradiation on the critical current has been studied since early 1990s [19–21], and continues to be relevant also at present time [22–24]. In [19] the dependences of the critical current on magnetic field, as well as on the irreversibility field, were measured. A rise (at all temperatures) of the irreversibility field (parallel to the anisotropy axis) under irradiation is shown. However, in the plane of the superconducting layers, the irreversibility field, on the contrary, decreases under irradiation. Suppression of the fishtail effect was observed for the critical current density. In [20] the effect of fast neutron irradiation on critical current $YBa_2Cu_3O_{7+\delta}$ was investigated. In the study [21], the molecular dynamics method combined with the Ginzburg–Landau theory was used to calculate the critical current in a magnetic field. For YBCO with columnar radiation defects, decreasing dependences of the critical current on the magnetic field are obtained. The influence of the regular and random distribution of defects was investigated.

Irradiation with a sufficiently high fluence lowers the critical temperature of the superconducting transition. In the study [22] the sample $YBa_2Cu_3O_{8+\delta}$ was irradiated with protons in such a way, that the resulting defects form a regular lattice. The local peaks of critical current, corresponding to the tuning fields, from the magnetic field are obtained. The distributions of the local critical temperature are obtained. In [23] the dependences of the critical current on the magnetic field were obtained for MgB_2, in [24] — for $La_{1.5}Dy_{0.5}CaBa_2Cu_5O_z$ (La-2125).

Studies of the effect of irradiation with heavy inert gas ions [25,26] show an insignificant rise of critical current at low fluences with a subsequent monotonic decrease up to the complete disappearance of superconducting properties already at the fluence $\sim 10^{17}\,m^{-2}$. As studies show, the radiation resistance of HTSC tapes to irradiation $^{132}Xe^{27+}$ (167 MeV), $^{132}Xe^{27+}$ (80 MeV) and $^{84}Kr^{17+}$ (107 MeV) is $1 \cdot 10^{12}\,cm^{-2}$, $35 \cdot 10^{12}\,cm^{-2}$ and $1 \cdot 10^{13}\,cm^2$ correspondingly. Also, the studies with the use of ions of various elements: oxygen [27–29], zirconium [30], lead [31], were carried out. It was shown that, under certain conditions, using the a beam of oxygen ions in the fields of the order 5 T a twofold increase in the critical current can be achieved.

In contrast to experiment, the numerical simulation allows to analyze in detail the pinning mechanism at the level of individual vortices and to separate the contribution of various factors to the formation of critical current. In the study [21], as well as in many others, a detailed numerical analysis of the influence of the concentration and location of defects on the critical current in a magnetic field was carried out. However, this was done for columnar defects corresponding to irradiation with high-energy ions. Numerical studies for radiation defects of other shapes are practically not covered in the literature.

The purpose of our study is to simulate the effect of some types of three-dimensional radiation defects arising at different irradiation energies on the pinning efficiency and HTSC critical current. We will consider the defects in the form of an amorphous track (columnar type of defects), point defects and cascade defects. A feature of our consideration is the direct consideration of the three-dimensional structure, which, as we will show, allows to simulate pinning on three-dimensional structural defects, namely, on rectilinear tracks, cascades and point defects. The article is structured as follows. Section 2 describes a model of a layered HTSC and explains a method for introducing a description of the interaction of a vortex with a radiation defect into the algorithm. Section 3 presents the results of calculating the dependence of the critical current on the magnetic field and their discussion. In the conclusion the main results of the study are described.

2. Model and calculation method

The calculations were performed by the Monte-Carlo method for a three-dimensional model of layered HTSC [32–35]. Within the framework of this model, a vortex filament is considered as a stack of plane interacting layer vortices — pancakes. The energy of the vortex system is as follows

$$G = \sum\Big\{N_z\varepsilon + \sum_{i<j} U_{in-plane}(r_{ij}) + \sum_{i,j} U_p(r_{ij}) + \sum_{i,j} U_{surf}\left(r_{ij}^{im}\right) + \sum_{i} U_{inter-plane}\left(r_i^{z,z+1}\right)\Big\},$$

where $\varepsilon = d\varepsilon_0(\ln[\lambda(T)/\xi T)] + 0.52)$ — vortex self-energy, $\lambda(0)$, $\xi(0)$ — penetration depth and coherence length at $T = 0$; N_z — number of pancakes in z plane; the second term describes the pairwise interaction of pancakes, the third — interaction of vortices with pinning centers, the fourth — interaction of vortices with the surface and Meissner and transport currents, the last — interplanar interaction of pancakes; $\varepsilon_0 = \Phi_0^2/(4\pi\lambda)^2$, $\Phi_0 = \pi\hbar c/e$ — magnetic flux quantum. For the interplanar interaction we used the potential shape obtained in the studies [36,37]:

$$U_{inter-plane}(r_i^{z,z+1}) = U_{em}(r_i^{z,z+1}) + U_{jos}(r_i^{z,z+1}),$$

U_{em} — electromagnetic, U_{jos} — Josephson interaction of pancakes located in adjacent layers. These terms are as follows

$$U_{em}(r_i^{z,z+1}) = 2d\varepsilon_0\lfloor C + \ln(r_i^{z,z+1}/2\lambda) + K_0(r_i^{z,z+1}/\lambda)\rfloor,$$

$C = 0.5772$ — Euler constant.

$$U_{jos}^{z,z+1}(r_i^{z,z+1}) = \begin{cases} \varepsilon_0 d[1+\ln(\lambda/d)]0.25(r_i^{z,z+1}/r_g)^2 \\ \qquad \times \ln(9r_g/r_i^{z,z+1}),\ r_i^{z,z+1} \le 2r_g, \\ \varepsilon_0 d[1+\ln(\lambda/d)][(r_i^{z,z+1}/r_g) - 0.5], \\ \qquad r_i^{z,z+1} > 2r_f, \end{cases}$$

$r_g = \gamma d$ — characteristic distance of the Josephson interaction, γ — anisotropy parameter, d — interplanar distance.

Due to computer speed and memory limitations in the Monte Carlo calculation, it is possible to consider a stack of no more than 20 planes. At the same time, the minimum HTSC film thickness used in practice — is about several hundreds of nm. As an output, we can combine several pancakes in adjacent planes and apply the subprocesses of birth, destruction and movement to the stack of pancakes as a single object. Approximately this approach is possible, since the real scale of the Abrikosov vortices bends is determined by the elastic parameters of the vortex filament [38] and is usually much larger than the interlayer distance. In our study a stack of 10 layer vortices is taken as a single object; thus, a system of 200 HTSC layers is considered.

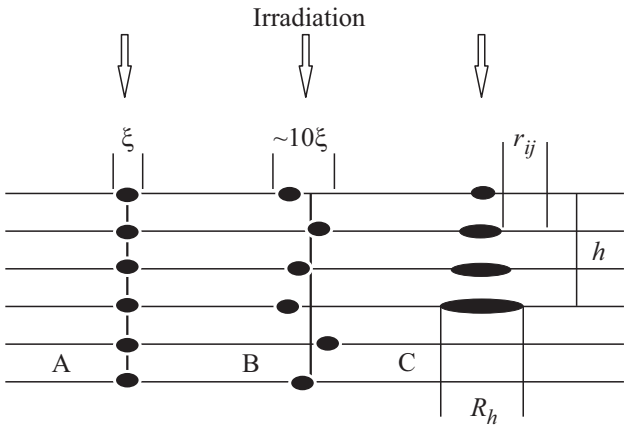

Figure 2. Schemes of radiation defects under irradiation with charged particles of various energies and electrons. The horizontal lines show HTSC layers. The direction of the defect axis coincides with the direction of radiation particles beam. *a* — Columnar defect (col-str in further figures), arises when irradiated with ions with energies from several hundred MeV to 1 GeV. *b* — A collection of point defects located randomly within a certain distance from the axis (col-rand in the following figures). Occurs when irradiated with electrons. *c* — Conical defect. It arises upon irradiation with ions with energies from several MeV to several tens of MeV. The vortex cannot penetrate inside the conical defect, but it can be fixed at the boundary.

Any superconductor always has structural defects, that act as pinning centers for vortices. Such defect is called intrinsic defect and is taken into account as a small area (of the order of the coherence length) with suppressed superconducting properties. In addition to its own pinning centers, the sample may contain artificial radiation defects. In our study, we investigate the effect on the vortex lattice of defects arising from the irradiation of a superconductor with electrons and ions of various energies, to be specific, with xenon ions [39]. The configurations of defects arising in this case are shown schematically in Fig. 2. If the ion energy is ~ 1 GeV, the defect has the form of a rectilinear track with the diameter $\sim \xi$, penetrating through the film (Fig. 2, *a*). If the ion energy is $\sim$ several MeV, the defect is not through and can be described as a cone expanding inward, the depth and radius of the base of which depend on the ion energy (Fig. 2, *c*). The radius in the lower part can reach λ. Let us assume, that such a defect is an area, where the vortex cannot penetrate, but can be fixed at the boundary. The pinning center arising from electron irradiation can be described as a collection of point defects located in each layer and at a random distance from the axis. Let us assume for definiteness, that this distance does not exceed 10ξ (Fig. 2, *b*). The defects corresponding to Fig. 2, *b* were considered in the study [22]. The superconductor also has its own random pinning centers with a radius of $\sim \xi$. The potential of vortex interaction with a defect is simulated

in the following way

$$U_{pm} = -\alpha \frac{1}{1 + r_{ij}/\xi} \exp\left(\frac{r_{ij}}{2\xi}\right),$$

where r_{ij} — the distance to the defect center or to the edge of the defect area for a conical defect (Fig. 2, *c*), α — the effective depth of the potential defect pit. This shape of potential well is taken to be the same for intrinsic and radiation defects. The depth of radiation defect pit is taken by an order greater than the depth of intrinsic defect pit (weak intrinsic pinning).

3. Results and discussion

For simulating we have chosen HTSC parameters based on bismuth $Bi_2Sr_2CaCu_2O_{8-\delta}$ (BSCCO, $\gamma(0) = 180\,\text{nm}$, $\xi(0) = 2\,\text{nm}$, $T_c = 84\,\text{K}$). Since the purpose of this study is to analyze the interaction of a vortex lattice with radiation defects, then to exclude thermal fluctuations effect we take $T = 1\,\text{K}$. The sample size in plane ab is $5 \times 3\,\mu\text{m}$, the film thickness is $c = 540\,\text{nm}$. In this case the sample contains on average about 1000 vortex filaments. As our previous calculations show, the results obtained for a small system can be qualitatively extrapolated to real experimental dimensions. The sample contains $N_h = 20$ radiation defects forming a triangular lattice. Conical radiation defects have a radius in the widest part $R_h = 200\,\text{nm}$ (this is greater than the depth of magnetic field penetration into the superconductor). The radius of a conical defect on the film surface — about ξ. This will not limit the generality of the conclusions, but will minimize the error associated with different possible locations of defects. The concentration of radiation defects was taken equal to $1.33 \cdot 10^{12}\,\text{m}^{-2}$), that corresponds by order of magnitude to HTSC radiation resistance under xenon irradiation.

Fig. 3 shows the calculated dependences of critical current on the magnetic field at different depths h of conical defects, depending on the energy of the irradiating ions. HTSC based on bismuth are highly anisotropic substances; therefore, in Fig. 3–4 the calculations are made with anisotropy parameter $\gamma = 250$.

It can be seen that at all magnetic field values, the critical current increases by about 30%. Moreover, deep defects are more effective at low fields.

Let us compare the efficiency of conical defects with the efficiency of columnar defects (col-str) and columnar ones with a scatter of individual point defects around its axis (col-rand, Fig. 4). In this calculation, the number of columnar straight defects and columnar defects with a scatter coincides with the number of conical ones and is equal to 20. In this case, the calculation shows, that in both strong and weak magnetic fields, an rise of critical current for columnar and random defects is on average about 10%, i.e. with equal fluence conical defects are more effective.

When passing to a superconductor with low anisotropy (YBCO, $\gamma = 10$) the replacement of specific lengths will not lead to qualitative changes. Therefore we will simply replace in our calculation $\gamma = 250$ with $\gamma = 10$. The results at an intermediate depth of defects are shown in Fig. 5. For the chosen configuration of intrinsic defects in the fields of the order of 1000 Gs it is possible to achieve an increase in the critical current by 1.5, while in a zero field the increase is about 40%.

Thus, at an equivalent concentration, conical defects are most effective for increasing the critical current, both in the strongly anisotropic and in the weakly anisotropic case. For a qualitative explanation of this result, let us further analyze

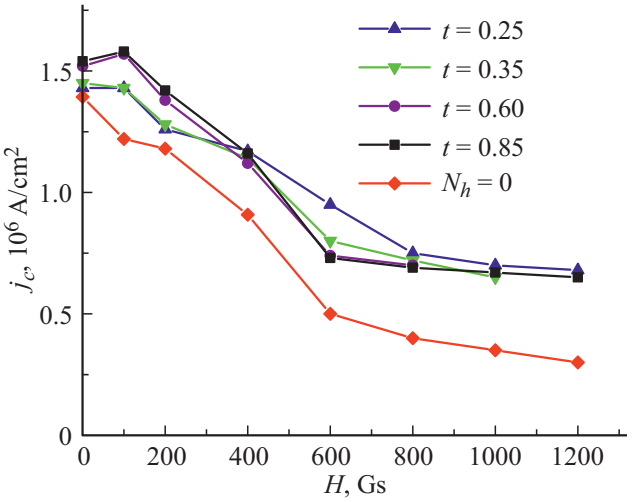

Figure 3. Dependence of the critical current on the defect depth. The parameter $t = h/c$ characterizes the relative depth of the conical defect. The absolute error of the critical current in this calculation is of the order of $0.01\,\text{A/cm}^2$ (estimated from three calculations, differing in the location of intrinsic defects).

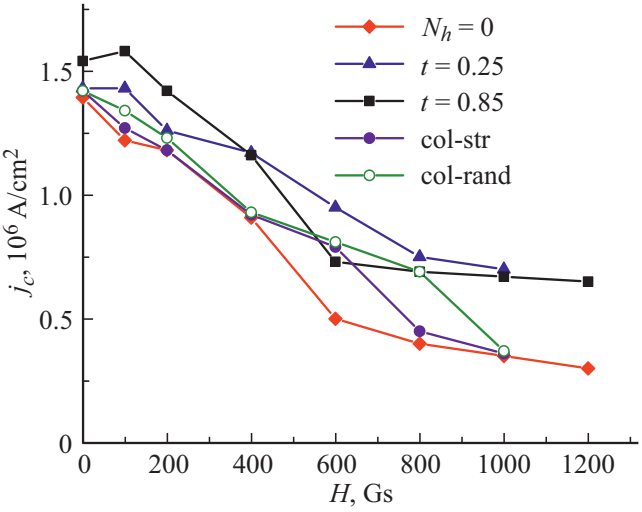

Figure 4. Comparison of critical current dependences on magnetic field for an unirradiated sample ($N_h = 0$) irradiated with the ions with two different values of conical defect relative depth, with radiation defects of type A (col-str) and type B (col-rand).

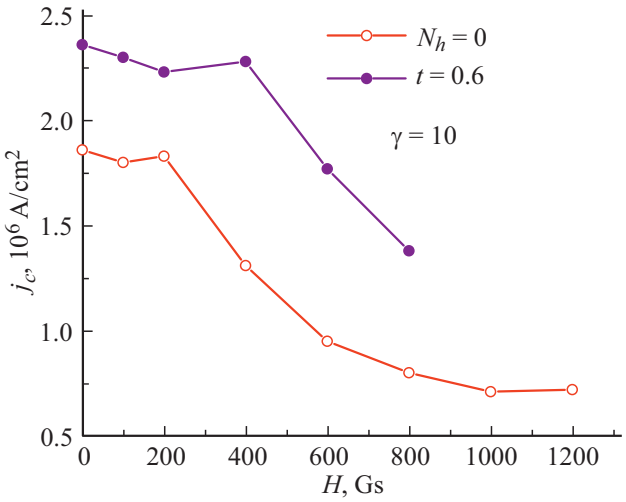

Figure 5. Critical current dependence on the magnetic field for conical defects, weakly anisotropic case. $N_h = 0$ — unirradiated superconductor, $t = 0.6-20$ conical defects with a relative depth $h/c = 0.6$.

the pinning of vortices on conical defects. To do this, we will take snapshots of the vortex structure with a current field slightly exceeding the first critical one, when there are not too many vortices in the sample. Let us consider the cases of low (YBCO) and high (BSCCO) anisotropy (Fig. 6). At low anisotropy, the vortex filament is rigid, so that such vortices either do not fix to defects at all, or the method of fixing corresponds to their minimal bending (and provides stronger pinning and critical current). Thus, rigid vortices are fixed on defects along the generatrix of the cone, that is additionally illustrated in ab plane top view. At high anisotropy multiple bends of vortices, partial fixing on the defect, vortex fixing simultaneously on several defects are observed, that results in the pinning decrease.

4. Conclusion

The interaction of a vortex lattice in a high-temperature superconductor with radiation defects is studied numerically, and the critical current and vortex configurations are calculated. The case of defects arising upon irradiation with ions of relatively low energy (several tens of MeV, conical defects) has been studied in detail. The following results were obtained.

1. The increase of critical current for conical defects is approximately 30%. With an equivalent irradiation fluence for conical defects the greatest increase of critical current is observed in comparison with columnar and random ones.

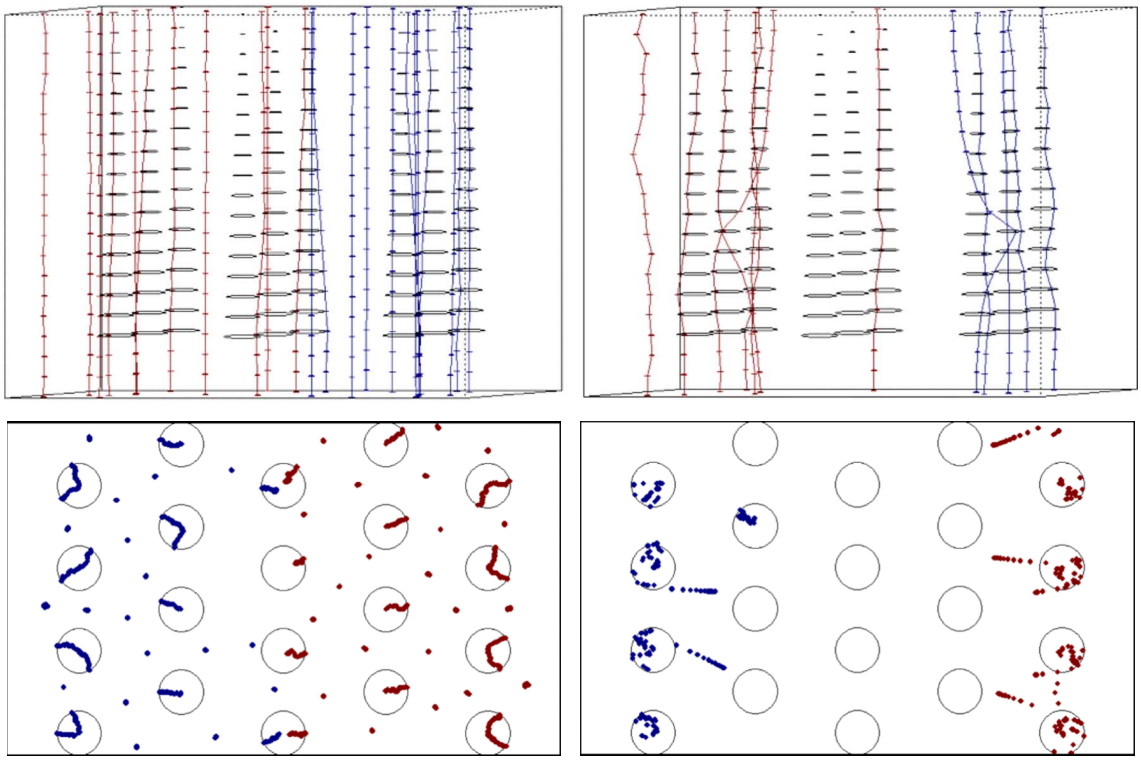

Figure 6. Vortex configurations arising during magnetization reversal by current, $t = 0.85$, no intrinsic defects. The upper figures show 3D vortex filaments interacting with conical defects. The circles of increasing radius denote the areas with suppressed superconductivity in each HTSC layer. In the lower figure (sample top view) the circles indicate the lower, widest parts of the defects. Red and blue colored circles — are pancakes. In order not to clutter up the figure, 3D configurations show fewer vortices and defects than the lower ones.

2. With a weak intrinsic pinning for a deep defect, weak growth in the critical current with increasing field is observed at low fields.

3. Irradiation with low-energy ions at an equivalent fluence increases the critical current by 10% for a superconductor with low anisotropy.

4. Deeper conical defects at low fields are more effective for enhancing pinning.

Work funding

The study was carried out with the financial support of the Russian Foundation for Basic Research under the scientific project No. 20-08-00811 (I.A. Rudnev), and also under financial support of Russian Foundation for Basic Research and state corporation „Rosatom“ within the framework of scientific project No. 20-21-00085 (V.A. Kashurnikov, A.N. Moroz).

Conflict of interest

The authors declare that they have no conflict of interest.

References

[1] J.S. Umezawa, G.W. Crabtree, J.Z. Liu, H.W. Weber, W.K. Kwok, L.H. Nunez, T.J. Moran, C.H. Sowers, H. Claus. Phys. Rev. B **36**, 7151 (1987).
[2] B.M. Vlcek, H.K. Viswananthan, M.C. Frischherz, S. Fleshler, K. Vandervoort, J. Downey, U. Welp, M.A. Kirk, G.W. Crabtree. Phys. Rev. B **40**, 67 (1993).
[3] J. Giapintzakis, W.C. Lee, J.P. Rice, D.M. Ginsberg, I.M. Robertson, M.A. Kirk, R. Wheeler. Phys. Rev. B **45**, 10677 (1992).
[4] M.K. Hasan, J. Shobaki, I.A. Al-Omari, B.A. Albiss, M.A. Al-Akhras, K.A. Azez, A.K. El-Qisari, J.S. Kouvel. Supercond. Sci. Technol. **12**, 606 (1999).
[5] L. Civale, A.D. Marwick, T.K. Worthington, M.A. Kirk, J.R. Thompson, L. Krusin-Elbaum, Y.R. Sun, J.R. Clem, F. Holtzber. Phys. Rev. Lett. **67**, 648 (1991).
[6] M.P. Smylie, M. Leroux, M. Mishra, L. Fang, M. Taddei, O. Chmaissem, W.K. Kwok. Phys. Rev. B, **93**, *11*, 115119 (2016).
[7] P. Biersack, L.G. Haggmark. Nucl. Instrum. Meth. Phys. Res. B **74**, 257 (1980). WWW.srim.org
[8] A.I. Podlivaev, I.A. Rudnev. FTT (in Russian) **63**, *6*, 712 (2021).
[9] M.C.H.W.W.M. Eisterer, R. Fuger, M. Chudy, F. Hengstberger, H.W. Weber. Supercond. Sci. Technol. **23**, *1*, 014009 (2009).
[10] M. Chudy, R. Fuger, M. Eisterer, H.W. Weber. IEEE Transact. Appl. Supercond. **21**, *3*, 3162 (2011).
[11] R. Prokopec, D.X. Fischer, H.W. Weber, M. Eisterer. Supercond. Sci. Technol. **28**, *1*, 014005 (2014).
[12] M. Jirsa, M. Rameš, I. Ďuran, T. Melíš ek, P. Kováč, L. Viererbl. Supercond. Sci. Technol. **30**, *4*, 045010 (2017).
[13] K.J. Leonard, F.A. List III, T. Aytug, A.A. Gapud, J.W. Geringer. Nucl. Mater. Energy, **9**, 251 (2016).
[14] D.X. Fischer, R. Prokopec, J. Emhofer, M. Eisterer. Supercond. Sci. Technol. **31**, *4*, 044006 (2018).
[15] J. Emhofer, M. Eisterer, H.W. Weber. Supercond. Sci. Technol. **26**, *3*, 035009 (2013).
[16] I.A. Rudnev, D.S. Odintsov, V.A. Kashurnikov. Phys. Lett. A, **372**, *21*, 3934 (2008).
[17] J. Trastoy, V. Rouco, C. Ulysse, R. Bernard, G. Faini, J. Lesueur, J. Briatico, J.E. Villegas. Physica C **506**, *15*, 195 (2014). http://dx.doi.org/10.1016/j.physc.2014.06.016
[18] N. Haberkorn, S. Suarez, S.L. Bud'ko, P.C. Canfield. Solid State Commun. **318**, 113963 (2020).
[19] M. Wacenovsky, R. Miletich, H.W. Weber, M. Murakami. Cryogenics **33**, *1*, 706 (1993).
[20] B. Shao, A. Liu, H. Ren, Q. He, L. Xiao, T. Takeyama. Mater. Res. Bull. **27**, *1*, 15 (1992).
[21] K. Takase, K. Demachi, K. Miya. Cryogenics **39**, *5*, 435 (1999).
[22] K.L. Mletschnig, W. Lang. Microelectron. Eng. **215**, 110982 (2019).
[23] V. Sandu, A.M. Ionescu, I. Ivan, L. Craciun, G. Aldica. Physica C **578**, 1353734 (2020).
[24] K.R. Mavani, D.S. Rana, S. Rayaprol, R.N. Parmar, D.G. Kuberkar, R. Kumar, R. Nagarajan. Solid State Commun. **142**, *8*, 462 (2007).
[25] G. Mikhailova, L. Antonova, A. Troitskii, A. Didyk, V. Malginov, T. Demikhov, E. Suvorova. Physica Status Solidi C, **10**, *4*, 677 (2013).
[26] A.V. Troitskii, L.K. Antonova, T.E. Demikhov, V.A. Skuratov, V.K. Semina, G.N. Mikhailova. Physica C **572**, 1353631 (2020).
[27] N. Haberkorn, S. Suárez, P.D. Pérez, H. Troiani, P. Granell, F. Golmar, S.H. Moon. Physica C **542**, *6*, 11 (2017).
[28] M. Leroux, K.J. Kihlstrom, S. Holleis, M.W. Rupich, S. Sathyamurthy, S. Fleshler, W.K. Kwok. Appl. Phys. Lett. **107**, *19*, 192601 (2015).
[29] S. Eley, M. Leroux, M.W. Rupich, D.J. Miller, H. Sheng, P.M. Niraula, L. Civale. Supercond. Sci. Technol. **30**, *1*, 015010 (2016).
[30] N. Haberkorn, S. Suárez, J.H. Lee, S.H. Moon, H. Lee. Solid State Commun. **289**, 51 (2019).
[31] I.A. Sadovskyy, Y. Jia, M. Leroux, J. Kwon, H. Hu, L. Fang, W.K. Kwok. Adv. Mater. **28**, *23*, 4593 (2016).
[32] W.E. Lawrence, S. Doniach. In: Proceedings of LT 12, Kyoto, 1970˜ Ed. E. Kanda. Keigaku, Tokyo (1971). 361 p.
[33] V.A. Kashurnikov, A.N. Maksimova, I.A. Rudnev, D.S. Odintsov. IEEE Transact. Appl. Supercond. **26**, *3*, 8200404, 1 (2016)
[34] V.A. Koshurnikov, A.N. Maksimova, I.A. Rudnev. FTT (in Russian) **56**, 861 (2014).
[35] A.N. Moroz, A.N. Maksimova, V.A. Kashurnikov, I.A. Rudnev. IEEE Trans. Appl. Supercond. **28**, 8000705 (2018)
[36] Sandeep Tyagi, Yadin Y. Goldschmidt. Phys. Rev. B **70**, 024501, 1 (2004)
[37] Yadin Y. Goldschmidt, Sandeep Tyagi. Phys. Rev. B **71**, 014503, 1 (2005)
[38] G. Blatter, M.V. Feigel'man, V.B. Geshkenbein, A.I. Larkin, V.M. Vinokur. Rev. Mod. Phys. **66**, *4*, 1125 (1994)
[39] E.I. Suvorova, P.N. Degtyarenko, I.A. Karateev, A.V. Ovcharov, A.L. Vasiliev, V.A. Skuratov, Ph.A. Buffat. J. Appl. Phys. **126**, 145106 (2019)